Vol. 46, No. 4 (2024) 589-595, DOI: 10.24874/ti.1694.05.24.07

Tribology in Industry

www.tribology.rs

RESEARCH

Optimization in Finite Elements to Define the Friction Factor Through Ring Compression Tests

Thomas G. Santos[a,*], André Rosiak[a], Diego R. Alba[b], Diego P. Wermuth[a], Lirio Schaeffer[a]

[a]*Universidade federal do Rio Grande do Sul, Av. Bento Gonçalves, 9500, Campus do Vale - Centro de Tecnologia, Bairro Agronomia 91509-900, Porto Alegre – RS, Brasil,*
[b]*Universität Stuttgart, Institut für Umformtechnik - Holzgartenstraße 17, 70174 Stuttgart, Deutschland.*

Keywords:

Ring compression test
Friction calibration curves
Friction factor
Cold forming
Optimization FEM analisys

* Corresponding author:

Thomas G. Santos
E-mail: thomas.santos@ufrgs.br

Received: 29 May 2024
Revised: 2 July 2024
Accepted: 26 July 2024

A B S T R A C T

The objective of this study was to evaluate the performance of a lubricant by defining the value of the friction factor at the interface. Ring compression tests were performed at room temperature for a typical steel in mechanical forming applications. The samples were compressed to 10%, 25% and 40% of their initial height with a constant speed of 3 mm/min. Using the FORGE NxT2.1 finite element software, an optimization procedure was carried out to reduce the computational cost, then simulations were performed by varying the values of the friction factor so that a cost function was minimized. The cost function for this optimization considers a relationship between the internal and external diameters of the specimens for the simulated and experimentally measured cases. The results showed a good relationship between experiments and numerical analysis. After the optimization was performed, the value of the friction factor m varied between 0.001078 and 0.0873, depending on the dimensional measurement method used.

1. INTRODUCTION

In most metal forming operations, friction at the interface between dies and generatrix has a significant effect on material flow, forming force and energy, surface finish of the formed component and die wear [1,2]. Additionally, the correct definition of friction parameters is an important input parameter for numerical analysis of forming processes. The Coulomb and Tresca laws are those traditionally used in simulation via the finite element method. They are presented, respectively, in equations 1 and 2:

$$\sigma_f = \mu\sigma_n \quad (1)$$

$$\sigma_f = m\tau \quad (2)$$

Onde: σ_f= Frictional stress [MPa]; μ= Coulomb friction coefficient [-]; σ_n= Normal Stress [MPa]; m= Tresca friction factor [adm.]; τ= Shear yield stress [MPa].

The prediction of friction stress made by one of these laws can be significantly different and the way to describe interfacial friction must be carefully selected respecting the nature of the

forming process. Both laws provide an estimate of the effects of friction rather than an exact prediction and may not be suitable for certain applications. For example, Coulomb's law overestimates friction in extrusion processes while Tresca's law fails to predict the region of adhesion close to the neutral point during lamination processes [3].

The most widespread method for identifying either the friction coefficient or the friction factor is the uniaxial ring compression test [4-7]. This method was first proposed by Kunogi [8] and was based on the idea of establishing a relationship between friction at the die/ring interface and the variation in the internal diameter of the ring during compression. It was shown that if interfacial friction is equal to zero, the ring should deform similarly to a solid disk, with each element flowing radially towards the outer region at a rate proportional to its distance from the center axis. As friction increases, it tends to restrict radial expansion. Thus, if friction exceeds a threshold, resistance to flow towards the outside becomes impossible and the flow of part of the material flows towards the center of the ring, as illustrated in Figure 1. Later, Male and Cockroft [9] experimentally obtained calibration curves for different values of friction coefficients, which demonstrate a relationship between the reduction in internal diameter and the reduction in ring height. These curves were widely used to define the coefficient of friction for various materials. However, it has recently been shown that the shape of the calibration curve can also be affected by material properties and therefore, it is recommended that individual curves be generated for each material [10,11].

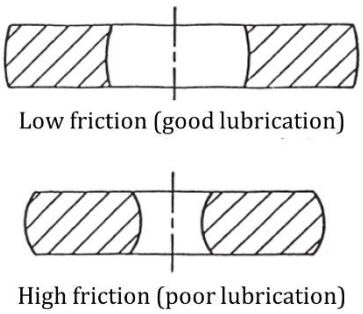

Fig. 1. Effect of friction on material flow during the ring compression test [10].

In recent decades, finite element analysis has provided an accurate prediction of material deformation and its geometric changes so that friction calibration curves can be created based on different friction conditions [12-14]. Additionally, in recent years, reverse analysis techniques in finite element methods with optimization algorithms to identify material and process parameters have been introduced [15-17]. In inverse analysis, the unknown parameters are determined from the minimization of a cost function based on experimental and numerical simulation results. FEA is used to analyze the behavior of the material during the experiment, while the optimization technique allows automatic adjustment of study parameters until the calculated response reaches the values measured during laboratory experiments within a pre-established tolerance range.

In this study, experiments based on compression testing were carried out on rings manufactured from LNE-380 steel and the value of the friction factor m was calculated for a commercially available lubricant.

2. EXPERIMENTAL PROCEDURE

Ring compression tests were conducted using specimens machined from laminated sheets of LNE-380 steel. LNE-380 steel presents good performance for cold forming processes, with a range of applications mainly in the manufacture of automotive components. A summary of the mechanical properties of this steel is shown in Table 1. The dimensions of the specimens follow the canonical geometry, 6:3:2, proposed for the ring compression test and can be seen in Figure 2.

Table 1. Mechanical properties of LNE-380 steel.

	YS [MPa]	UTS [MPa]	E [%]
LNE-380	380~540	460~620	20

YS=Yeld strength; UTS=Ultimate tensile strength; E=Elongation.

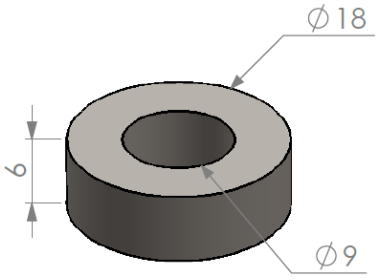

Fig. 2. Dimensions in millimeters of the test specimens for the ring compression test.

As a lubricant, the highly refined basic mineral oil Neutron Super Corte 1123 21S was used. This lubricant is specially developed for drawing operations in materials where there is a need for high pressure oil additives. The specimens were completely immersed in the lubricant, ensuring uniform surface coverage before being placed into the flat dies to begin compression.

For the tests, an EMIC Universal Testing machine with a capacity of 600 kN was used. The tests were carried out at a constant speed of 3 mm/min. Flat bases with a diameter of 155 mm made of AISI-H13 Hot Working Steel with a hardness close to 55 HRC were used as matrices for the experiments. The tests were carried out at room temperature and the lubrication procedure included careful cleaning of the matrices with isopropyl alcohol to remove impurities and subsequent deposition of the lubricant on the flat faces of the matrix. Subsequently, the test specimens were immersed in the lubricant and placed on the matrices.

The reductions used were 10%, 25% and 40% of the initial height of the specimen. For each reduction, 3 specimens were tested in order to provide greater reliability for the experimental data. Before and after the experiments, the heights of the specimens were measured using a micrometer and a caliper was used to measure the internal and external diameter. In each case, for greater precision, an average of three measurements was taken as the final value given the fact that the deformation of the specimens does not occur uniformly, leading to the internal part having an ellipsoid shape. As an alternative to diameter measurements, a methodology using image analysis (IA) was carried out and compared to manual measurements (M) carried out using a centesimal caliper.

For this alternative methodology, measurements of the internal and external diameters of the specimens were carried out by capturing images with high contrast and 600 dpi resolution. These were subsequently treated using the free software ImageJ©. The method used for the analysis is presented in Figure 3.

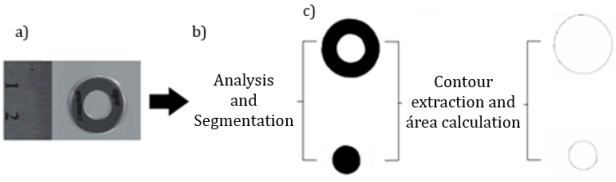

Fig. 3. Methodology used to measure diameters by image analysis.

The captured images were previously calibrated in the software resulting in a ratio of 24 pixels/mm (Figure 3a). Subsequently, these were segmented and their internal and external contours were extracted to define their respective areas (Figure 3b and Figure 3c). Using the values of the areas, the values of the equivalent diameters were determined using Equation 3.

$$D_{eq} = \sqrt{\frac{A}{\frac{\pi}{4}}} \tag{3}$$

Where: D_{eq}= Equivalent diameter [mm]; A= Area of the segmented figure [mm^2].

2.1 Finite element analysis

For numerical simulations in finite elements, FORGE NxT2.1 software was used and boundary conditions closest to the experiments were considered. In order to reduce the computational effort, the model adopted was 2D-elastoplastic where the matrices were considered rigid bodies. The dimensions of the test piece follow those shown in Figure 2. The flow curve of the LNE-380 steel material was introduced into the software through the analytical equation according to Hollomon's Law as shown in Equation 4:

$$k_f = 927.8\,\varphi^{0.1755} \tag{4}$$

Where k_f= Yield Stress [MPa]; φ= Equivalent plastic strain [mm/mm].

Table 2. Input parameters for the finite element model.

Mesh Size	0.25 mm
Element type	Tetrahedral
Number of elements	4551
Initial temperature	20°
Ambient temperature	20°C
Convection heat exchange coefficient	Adiabatic
Conduction heat exchange coefficient	Adiabatic
Emissvity	0.88
Friction between generator/dies	m=0.5
Press type	Hydraulic
Press speed	3 mm/min
Strain	Approximately 40% of the initial height of the specimen*

The flow curve of LNE-380 was obtained through compression tests on three cylindrical specimens. Table 2 describes the other input parameters for the model.

It is worth noting that the value assigned to parameter m is only an initial analysis assumption. For the optimization procedure that aims to define this parameter, an analysis is carried out which seeks to adjust the internal and external radii between the experimental measurements and simulated results. For this analysis, the optimization package included in the software automatically runs compression simulations by varying the friction factor and friction coefficient until the cost function, Equation 5, is minimized [16].

$$F_{custo} = \frac{|r_{int\,FEA} - r_{int\,exp.}|}{1+|r_{int\,FEA} - r_{int\,exp.}|} + \frac{|r_{ext\,FEA} - r_{ext\,exp.}|}{1+|r_{ext\,FEA} - r_{ext\,exp.}|} \quad (5)$$

Where F_{custo}= Cost function [adm.]; $r_{int\,FEA}$= internal radius from the finite element simulation [mm]; $r_{int\,exp}$= internal radius from the experiments [mm]; $r_{ext\,FEA}$= external radius from the finite element simulation [mm]; $r_{ext\,exp}$= external radius from the experiments [mm].

3. RESULTS AND DISCUSSIONS

The tested samples are shown in Figure 4. Among these, all showed an increase in internal diameter, demonstrating low values of friction at the interface.

Table 3 presents the results of height, internal diameter and external diameter measurements for each sample. Additionally, the average values for each of the reductions carried out are presented.

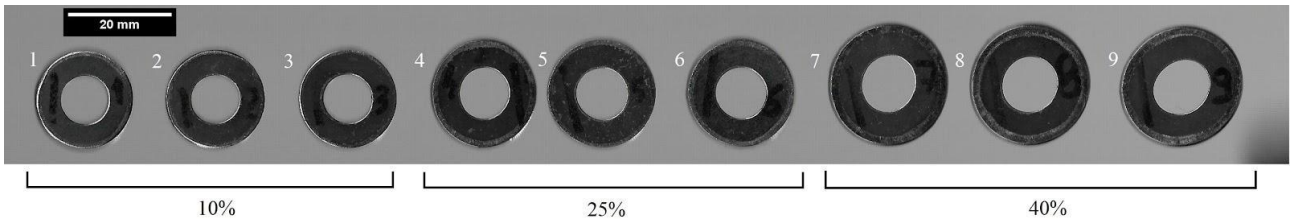

Fig. 4. Samples from compression tests.

Table 3. Geometry results after compression testing through manual measurement.

Samples	Height Reduction [%]	h_{final} [mm]	$Ø_{int\ final}$ [mm]	$Ø_{ext\ final}$ [mm]	Height true reduction h [%]	Internal true reduction $Ø_{int}$ [%]	External True reduction $Ø_{ext}$ [%]
1	10%	5.47	9.21	19.12	9.03	-3.56	-6.11
2	10%	5.49	9.16	18.95	8.45	-1.59	-5.28
3	10%	5.44	9.21	18.92	8.97	-1.84	-5.00
Average	10%	5.46	9.19	18.96	8.82	-2.33	-5.46
4	25%	4.44	9.56	20.81	25.65	-5.90	-15.56
5	25%	4.52	9.70	20.90	24.61	-7.85	-16.11
6	25%	4.50	9.77	21.13	25.15	-8.71	-17.22
Average	25%	4.49	9.68	20.95	25.14	-7.49	-16.30
7	40%	3.55	10.17	23.62	40.84	-13.08	-31.11
8	40%	3.58	10.10	23.35	39.45	-12.85	-29.72
9	40%	3.55	11.02	23.35	39.80	-22.68	-29.72
Average	40%	3.56	10.43	23.44	40.03	-16.20	-30.18

Table 4. Geometry results after compression testing through image analysis.

Samples	Height reduction [%]	Internal area [mm²]	$Ø_{int}$ [mm]	External area [mm²]	$Ø_{ext}$ [mm]	Internal true reduction $Ø_{int}$ [%]	External true reduction $Ø_{ext}$ [%]
1	10%	67.12	9.24	282.76	18.97	-3.95	-5.38
2	10%	65.66	9.14	275.32	18.72	-1.41	-4.00
3	10%	64.46	9.06	273.08	18.65	-0.22	-3.61
Average	10%	65.75	9.15	277.06	18.78	-1.84	-4.33
4	25%	82.70	10.26	329.83	20.49	-13.66	-13.83
5	25%	82.71	10.26	329.04	20.47	-14.07	-13.72
6	25%	82.63	10.26	334.48	20.64	-14.09	-14.67
Average	25%	82.68	10.26	331.12	20.53	-13.93	-14.06
7	40%	109.25	11.79	409.42	22.83	-31.14	-26.83
8	40%	100.99	11.34	407.19	22.77	-26.70	-26.50
9	40%	104.95	11.56	409.34	22.83	-28.72	-26.83
Average	40%	105.06	11.57	408.65	22.81	-28.87	-26.72

Table 4 presents the values for calculating the average diameters through the image analysis procedure.

Figure 5 shows the values of the reductions in height and internal diameter plotted on the calibration curves generated through the finite element software. The results of the optimization procedure are also plotted in Figure 5.

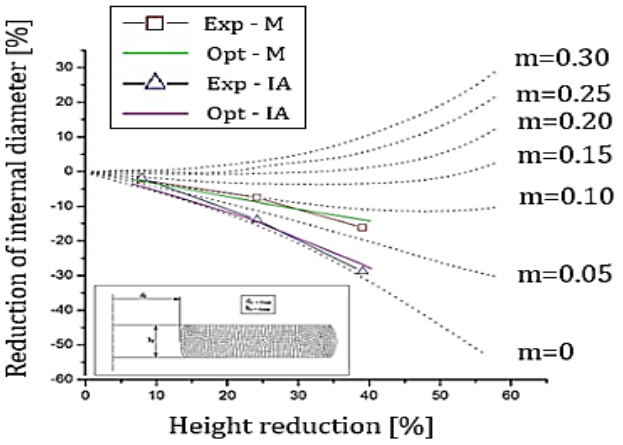

Fig. 5. Calibration curves for LNE-380 steel for friction factor m.

A summary of the last five iterations performed during the optimization procedure is shown in Table 5. The second column of the table shows the results of the calculated cost function.

Table 5. Results of the optimization procedure for manual geometry measurements after compression testing.

Case	Cost function	Øint [mm]	Øext [mm]	Friction factor m
1	0.1095	10.170	22.608	0.0873
2	0.1099	10.168	22.606	0.0874
3	0.1104	10.175	22.608	0.0870
4	0.1106	10.166	22.605	0.0876
5	0.1111	10.178	22.610	0.0868

The closer this value is to zero, the better the fit between the numerical model and experimental measurements. Subsequently, the values of the internal and external diameters are shown. The relative error between simulation and experiments was 2.49% for the internal diameter and 3.55% for the external diameter. Finally, the last column presents the values of m used for each iteration. In this way, the optimization shows that the value of the friction factor at the interface that best fits the experiments is m= 0.0873. These friction conditions are quite low and show the efficiency of the lubricant chosen for the analysis.

Following the same procedure, Table 6 shows the results of the optimizations for the analysis which considers diameter measurements through image analysis of the specimens. In this case, the relative error between simulation and experiments was 0.08% for the internal diameter and -1.48% for the external diameter. The optimization shows that the value of the friction factor at the interface that best fits the experiments is m= 0.001078.

Table 6. Results of the optimization procedure for measurements through image analysis of geometries after compression testing.

Case	Cost function	Øint [mm]	Øext [mm]	Friction factor m
1	0.0548	11.561	23.147	0.001078
2	0.0550	11.563	23.147	0.000950
3	0.0553	11.559	23.146	0.001217
4	0.5564	11.558	23.145	0.001331
5	0.0559	11.566	23.149	0.000784

Finally, the force-displacement curve from the experiments was compared with the curve obtained through simulation for the optimized cases. Figure 6 shows that the simulated values are a good approximation to those acquired during the test. For the experiments, the maximum force values were close to 340 kN while for the optimized cases they were 264 kN and 290 kN. The largest relative difference between measured and simulated values is 22%.

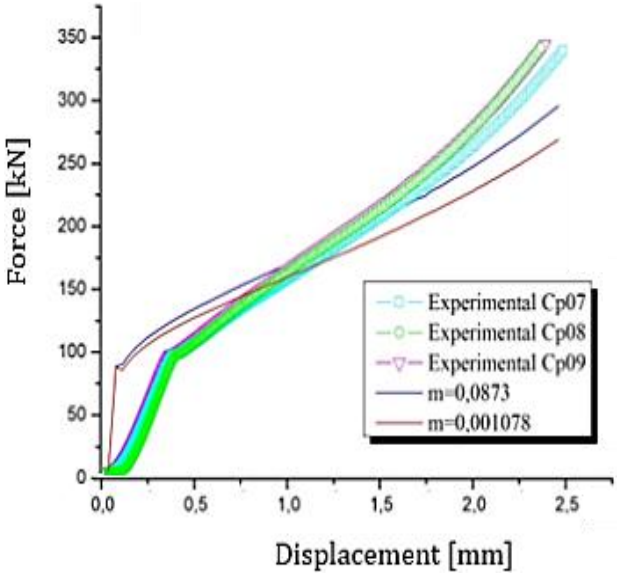

Fig. 6. Force [kN] per Displacement [mm] graph for the three tested samples and for the two numerical optimization simulations. Reduction in height of 40%.

4. CONCLUSION

Ring compression tests were carried out on samples of LNE-380 steel to obtain the values of the friction factor and coefficient of friction for the industrial lubricant Neutron Super Corte 1123 21S during cold forming processes. Based on the experimental results, finite element optimization simulations were carried out to compare and validate the results. Based on the results presented in this work, the following conclusions can be presented:

- The values referring to the friction factor m depend on the method used to define the variation in the internal and external diameter of the sample. When using the usual method of measuring using a caliper, for a height reduction of 40%, the internal diameter presents a value of 10.43 mm, resulting in a percentage reduction of -16.20% relative to its initial diameter. The external diameter, in turn, has an average value of 23.44 mm resulting in a reduction of -30.18%. Using image analysis, which seeks to provide greater precision by suppressing the ellipse-shaped deformation effect, the average internal diameter and reduction values are respectively 11.56 mm and -28.87%. For the external diameter these values are respectively 22.81 mm and -26.72%.
- An optimization package included in the finite element software was used to define the value of the friction factor for the cases analyzed through manual measurements and image analysis. For the manual measurement methodology using calipers, the value of the friction factor m was 0.0873. For the methodology involving image analysis, the optimization simulations resulted in a value for the friction factor m of 0.001078.
- The relative difference between the dimensions, for the optimizations, when comparing the final geometries of the experiments and simulations was less than 3.6%.
- Comparing the Force Displacement curves between experiments and numerical analyzes the maximum difference is less than 22%.
- The methodology presented here serves as a basis for defining friction parameters that aim to feed numerical simulations of cold forming processes. If a more conservative analysis is desired, overestimating the forming energy, the friction values from manual measurements can be used. If a less conservative approach is desired, underestimating the forming energy, the values of the friction parameters derived from the image analysis methodology can be used.
- New experiments for different reductions in specimen height, different specimen dimensions and deformation speeds must be carried out to validate the results obtained in this work.

Acknowledgement

This study was financed in part by the Conselho Nacional de Desenvolvimento Científico e Tecnológico – Brasil (CNPq) – Finance Code CNPq/MCTI/FNDCT nº 18/2021 (Process: 404196/2021-7). The authors are recipients of fellowships from the CNPq (research productivity – PQ1-4/2021; PDJ – 25/2021; GD – 2019) and CAPES (PROEX-IES-2020).

REFERENCES

[1] F. Klocke, *Manufacturing Processes 4*, 2013, doi: 10.1007/978-3-642-36772-4.

[2] K. Lange et al., "Handbook of Metal Forming," *Journal of Applied Metalworking*, vol. 4, no. 2, p. 188, Jan. 1986, doi: 10.1007/bf02834383.

[3] Joun, H. G. Moon, I. S. Choi, M. C. Lee, and B. Y. Jun, "Effects of friction laws on metal forming processes," *Tribology International*, vol. 42, no. 2, pp. 311–319, Feb. 2009, doi: 10.1016/j.triboint.2008.06.012.

[4] J. Rodrigues and P. Martins, *Livro Tecnologia Mecânica - Vol. I - 2a edição,* Escolar, 2010.

[5] L. Schaeffer, *Manufatura por conformação mecânica*, Impressa Livre, 2006.

[6] T. Altan, S.-I. Oh, and H. L. Gegel, "Metal Forming : Fundamentals and applications", CiNii Books, 1983, [Online], Available: https://ci.nii.ac.jp/ncid/BA12627038

[7] P. R. B. Júnior, V. Martins, and L. Schaeffer, "Determinação do coeficiente de atrito pelo ensaio de compressão do anel: uma revisão," *Revista Thema*, 2011. [Online], Available: https://doaj.org/article/5fa78feb8bb24a599ae8fd8398974808.

[8] M. Kunogi, "A new method of cold extrusion," *Transactions of the Japan Society of Mechanical Engineers*, vol. 23, no. 134, pp. 742–749, Jan. 1957, doi: 10.1299/kikai1938.23.742.

[9] A. T. Male and M. G. Cockcroft, "A method for the determination of the coefficient of friction of metals under conditions of bulk plastic deformation," *Wear*, vol. 9, no. 3, p. 241, May 1966, doi: 10.1016/0043-1648(66)90161-x.

[10] H. Sofuoglu, H. Gedikli, and J. Rasty, "Determination of friction coefficient by employing the ring compression test," *Journal of Engineering Materials and Technology*, vol. 123, no. 3, pp. 338–348, Sep. 2000, doi: 10.1115/1.1369601.

[11] A. M. Camacho, A. I. Torralvo, C. Bernal, and L. Sevilla, "Investigations on friction factors in metal forming of industrial alloys," *Procedia Engineering*, vol. 63, pp. 564–572, Jan. 2013, doi: 10.1016/j.proeng.2013.08.240.

[12] E. Rajesh and S. Muthukrishnan, "Analysis of friction factor by employing the ring compression test under different lubricants," *International Journal of Scientific & Engineering Research,* vol. 4, iss. 5, Jun. 2021.

[13] M. Dehghan, F. Qods, M. Gerdooei, and J. Doai, "Analysis of ring compression test for determination of friction circumstances in forging process," *Applied Mechanics and Materials*, vol. 249–250, pp. 663–666, Dec. 2012, doi: 10.4028/www.scientific.net/amm.249-250.663.

[14] I. Equbal, P. ALAM, R. Ohdar, and S. Alam, "IJMPE studies on lubrication behavior of 35C8 steel using ring compression test and finite element simulation," *International Journal of Mechanical and Production Engineering*, vol. 4, no. 11, pp. 4–8, Nov. 2016.

[15] H. Cho and T. Altan, "Determination of flow stress and interface friction at elevated temperatures by inverse analysis technique," *Journal of Materials Processing Technology*, vol. 170, no. 1–2, pp. 64–70, Dec. 2005, doi: 10.1016/j.jmatprotec.2005.04.091.

[16] S. Marie, R. Ducloux, P. Lasne, J. Barlier, and L. Fourment, "Inverse analysis of forming processes based on FORGE environment," *Key Engineering Materials*, vol. 611–612, pp. 1494–1502, May 2014, doi: 10.4028/www.scientific.net/kem.611-612.1494.

[17] I. Pérez and A. Mangas, Eds., *Forging preforms design and inverse analysis for friction coefficient calculation by means of FORGE Optimization Tool.* 2017.